Journal of Catalysis 261 (2009) 50–59

Contents lists available at ScienceDirect

Journal of Catalysis

www.elsevier.com/locate/jcat

Kinetics and selectivity of methyl-ethyl-ketone combustion in air over alumina-supported PdO_x–MnO_x catalysts

G. Arzamendi [a], V.A. de la Peña O'Shea [b,1], M.C. Álvarez-Galván [b], J.L.G. Fierro [b], P.L. Arias [c], L.M. Gandía [a,*]

[a] Departamento de Química Aplicada, Edificio de los Acebos, Universidad Pública de Navarra, Campus de Arrosadía s/n, E-31006 Pamplona, Spain
[b] Instituto de Catálisis y Petroleoquímica, CSIC, Cantoblanco, 28049 Madrid, Spain
[c] Departamento de Ingeniería Química y del Medio Ambiente, Escuela Técnica Superior de Ingeniería de Bilbao, UPV/EHU, Alameda de Urquijo s/n, 48013 Bilbao, Spain

ARTICLE INFO

Article history:
Received 13 August 2008
Revised 22 October 2008
Accepted 3 November 2008
Available online 22 November 2008

Keywords:
Methyl-ethyl-ketone (MEK)
Palladium oxides
Manganese oxides
Bimetallic Pd–Mn catalysts
Catalytic combustion
Kinetics
Selectivity
VOCs

ABSTRACT

A study is presented of the kinetics and oxidation selectivity of methyl-ethyl-ketone (MEK) in air over bimetallic PdO_x(0–1 wt% Pd)–MnO_x(18 wt% Mn)/Al_2O_3 and monometallic PdO_x(1 wt% Pd)/Al_2O_3 and MnO_x(18 wt% Mn)/Al_2O_3 catalysts. Reaction rate data were obtained at temperatures in the 443–523 K range and for MEK partial pressures in the reactor feed of between 6.5 and 126.6 Pa. Products of both MEK combustion and partial oxidation reactions were found. Monometallic Pd/Al_2O_3 was the most selective catalyst for complete oxidation whereas the partial oxidation of MEK in the presence of manganese oxides was significant. The maximum yield for the partial oxidation products (acetaldehyde, methyl-vinyl-ketone, and diacetyl) was always below 10%. Kinetic studies showed that the rates of CO_2 formation over PdO_x/Al_2O_3 were well-fitted by the surface redox Mars–van Krevelen (MvK) kinetic expression and also by a Langmuir–Hinshelwood (LH) model derived after considering the surface reaction between adsorbed MEK and oxygen as the rate-determining step. In the case of the Mn-containing catalysts the MvK model provides the best fit. Irrespective of the model, the kinetic parameters for the bimetallic Pd–Mn catalysts were between the values obtained for the monometallic samples, suggesting an additive rather than a cooperative effect between palladium and manganese species for MEK combustion.

1. Introduction

Catalytic combustion offers interesting advantages over conventional flame combustion. It can be carried out at low temperature, thereby reducing or even avoiding the use of auxiliary fuel, as well as reducing the formation of thermal NO_x. Moreover, catalytic combustion is feasible at any fuel-to-oxidant ratio thus allowing for the treatment of streams containing very low concentrations of hydrocarbons [1]. There is growing interest in this technology for the production of electricity with natural gas turbines, as well as for the abatement of pollutant volatile organic compounds (VOCs) [2]. Although there are a wide variety of active catalysts in combustion reactions, two main groups can be distinguished: noble metals (mainly Pt and Pd) and transition metal oxides (Co, Cr, Cu, Mn and Ni) that can be present as single or mixed oxides (perovskites, espinels and hexaaluminates). These catalysts may have very different performances as concerns their activity or ability to start the ignition of a given VOC at low temperature, selectivity, thermal stability and resistance to water or to deactivation by any other compound present in the feed stream [3–5].

The so-called ignition or light-off curves constitute the most widely used manner for evaluating catalytic performance in hydrocarbon combustion studies. They are conversion-reaction temperature graphs obtained by measuring the fuel or VOC conversion as the reaction temperature is changed, which typically results in a sigmoid or S-shaped curve [6]. It is thereby possible to determine the minimum space–time (or amount of catalyst) required to achieve the complete combustion of the organic compounds contained in a given gas stream at a sufficiently low temperature. Nevertheless, the suitably design of a combustion reactor requires knowing the kinetics of the reaction over the selected catalyst. At present, there is a considerable amount of information in the literature based on light-off results, whereas kinetic and selectivity studies are generally scarce.

Methyl-ethyl-ketone (MEK, 2-butanone) is a ketone widely used as solvent in many industrial applications; however, it is hazardous and its emission to the atmosphere has to be controlled according to environmental regulations [7]. Catalytic combustion is a suitable and relatively simple technology for controlling the emissions of this VOC [8]. Nevertheless, to the best of our knowledge, there are only four previous studies on the kinetics of the catalytic combus-

* Corresponding author. Fax: +34 948 169606.
E-mail address: lgandia@unavarra.es (L.M. Gandía).
[1] Present address: Instituto Madrileño de Estudios Avanzados en ENERGIA, C/Tulipán s/n, 28933 Móstoles, Madrid, Spain.

0021-9517/$ – see front matter
doi:10.1016/j.jcat.2008.11.001

tion of MEK. The catalysts considered in these works were metallic foams [8], Fe_2O_3 [9], Cr/ZrO_2 [10] and Pt/Al_2O_3 [11].

This paper studies the combustion of MEK over mono and bimetallic alumina-supported Pd–Mn catalysts. The combinations of certain noble metals (mainly Ag, Pd or Pt) and manganese have been reported to improve catalytic performance, thermal stability and resistance to deactivation by poisoning. Previous studies with $Pd–Mn/Al_2O_3$ catalysts revealed a synergistic effect between MnO_x and PdO_x species resulting in a remarkable improvement in the activity for the complete oxidation of formaldehyde, methanol [12–14] and methane [15,16]. The aim of this study is to investigate the performance of Pd–Mn catalysts in the combustion of MEK, with emphasis in the kinetics and selectivity; issues that have hitherto received little attention.

2. Experimental

2.1. Catalysts preparation

A commercial γ-alumina powder (PURALOX HP-14/150, CONDEA) was used as a carrier to prepare manganese and palladium oxide catalysts. Before the incorporation of Mn and Pd, this support was dried at 423 K and calcined at 1073 K for 4 h. The Mn-containing catalyst (MnA, where A refers to the alumina support), with a manganese loading of 18 wt%, was prepared by impregnation with the appropriate volume (4 ml of solution per gram of support) of an aqueous solution of manganese nitrate ($Mn(NO_3)_2{\cdot}4H_2O$, Panreac, reagent grade). Excess water was removed in a rotary evaporator at 353 K for 2 h. This catalyst precursor was then dried at 383 K for 4 h and calcined in static air at 773 K for 4 h. Aliquots of this catalyst were subsequently used to prepare the bimetallic Mn–Pd catalysts. Suitable amounts of palladium nitrate were employed for this purpose. The procedure was the same as above described for the raw monometallic Mn catalyst. Three binary palladium-manganese catalysts were thus prepared by consecutive impregnation of the manganese sample with aqueous solutions of $Pd(NO_3){\cdot}H_2O$ (Fluka, reagent grade). The volume of solution was selected to achieve a final content of 0.25, 0.50 and 1.0 wt% Pd. The dried impregnates were calcined in air at 773 K for 4 h. These binary catalysts will be referred to hereafter as *x*PdMnA (where *x* stands for the palladium loading as wt%). A monometallic alumina-supported palladium catalyst containing 1.0 wt% Pd (PdA) was also prepared according to the same procedure followed in the bimetallic systems.

2.2. Catalysts characterization

Elemental analysis was performed by Inductively Coupled Plasma Atomic Emission Spectroscopy (ICP-AES) using a Perkin–Elmer optima 3300 DV spectrophotometer. Specific surface areas were calculated using the BET method from the nitrogen adsorption isotherms, recorded at the temperature of liquid nitrogen at atmospheric pressure (77 K) on a Micromeritics apparatus, model ASAP-2000, taking a value of 0.162 nm^2 for the cross-sectional area of the N_2 molecule adsorbed at 77 K. Prior to the adsorption measurements, samples were degassed at 413 K for 2 h.

The phase composition of the calcined samples was analyzed by X-ray diffraction (XRD) using a PANalytical X'Pert Pro Diffractometer operating with the following parameters: Cu K_α radiation ($\lambda = 1.5405$ Å), 45 mA, 40 kV, Ni filter, 2θ scanning range 5–80°, and scan step size of 0.03. Phase identification was made using the reference database supplied with the equipment.

Photoelectron spectra (XPS) of the fresh and used catalysts were acquired with a VG Escalab 200R spectrometer equipped with a hemispherical electron analyzer and an Al $K_{\alpha 1}$ ($h\nu = 1486.6$ eV, 1 eV $= 1.6302 \times 10^{-19}$ J) 120 W X-ray source. The powder samples were placed in a pretreatment chamber and degassed at 573 K. All binding energies (BE) were referred to Al 2p line at 74.5 eV.

Table 1
Chemical composition and BET specific surface area of alumina-supported mono- and bimetallic Mn–Pd samples.

Catalyst	Mn (wt%)	Pd (wt%)	S_{BET} (m^2/g)
MnA	16.3	0	33.9
0.25PdMnA	14.3	0.25	36.7
0.50PdMnA	14.9	0.49	31.9
1PdMnA	15.1	0.92	38.3
PdA	0	0.92	77.2

2.3. Catalytic performance

The MEK combustion reaction was carried out at atmospheric pressure in a tubular (8 mm i.d.) fixed-bed Pyrex glass reactor. Mass flow controllers (Bronkhorst) monitored and controlled the flow of gases used to obtain the feed mixture and pretreat the catalyst. Two types of catalytic tests were carried out to obtain the light-off curves and the kinetic runs. In the case of the light-off experiments, the catalyst (0.10 g) was diluted with 0.20 g of inert solids (Pyrex glass beads, 0.1–0.2 mm) forming a bed of about 10–12 mm in length. A thermocouple placed inside the reactor, in the center of the catalyst bed, monitored the reaction temperature. Prior to each experiment, the catalyst was treated under 100 $cm^3\,min^{-1}$ (STP) of air (Praxair 99.999%) for 1 h at 673 K. The total feed flowrate was 550 $cm^3\,min^{-1}$ (STP) with a MEK partial pressure of 126.6 Pa (1250 ppmv), resulting in a weight hourly space velocity (WHSV) referred to the amount of supported catalyst in the reactor and total feed mass flowrate of 425 h^{-1}. The ignition curves were obtained after pretreatment in the decreasing temperature mode starting from 673 K. The kinetic experiments were conducted at constant temperature and the reactor operated in the differential regime (MEK conversion <15%). After pretreatment, the catalytic bed was allowed to cool down in order to reach the temperature of the kinetic test (443–523 K). MEK partial pressure in the reactor feed was varied between 6.5 and 126.6 Pa (64–1250 ppmv). Online analysis of the product stream was performed on a Hewlett Packard 6890 gas chromatograph, equipped with a 6 ft HayeSep Q column connected to a TCD for CO_2 determination, and an HP-INNOWax 30 m × 0.32 mm i.d. column connected to an FID for MEK and partial oxidation products: acetaldehyde, acetic acid, methyl-vinyl-ketone and diacetyl (2,3-butanedione) analyses.

3. Results and discussion

3.1. Catalysts characterization

3.1.1. Chemical analysis, specific surface area and XRD

The chemical analysis of both manganese and palladium was performed by ICP-AES, with the analytical values being very close to the nominal ones. Both chemical composition and specific BET surface areas are compiled in Table 1. BET surface areas decrease with respect to the bare alumina support ($S_{BET} = 79.9$ m^2/g) upon manganese and palladium incorporation, with this decrease being much higher after manganese introduction, since the high manganese load should give way to big crystallites that may occlude the mouth of the support pores, thus producing a substantial decrease in surface area. The BET surface areas obtained for bimetallic catalysts show that the incorporation of such small amounts of palladium to the Mn-loaded sample as well, as to the bare alumina, did not substantially alter the specific surface area.

The crystalline phases of the mono and bimetallic alumina-supported catalysts were studied by XRD (Fig. 1). The crystalline phases found in the calcined alumina before metal impregnation

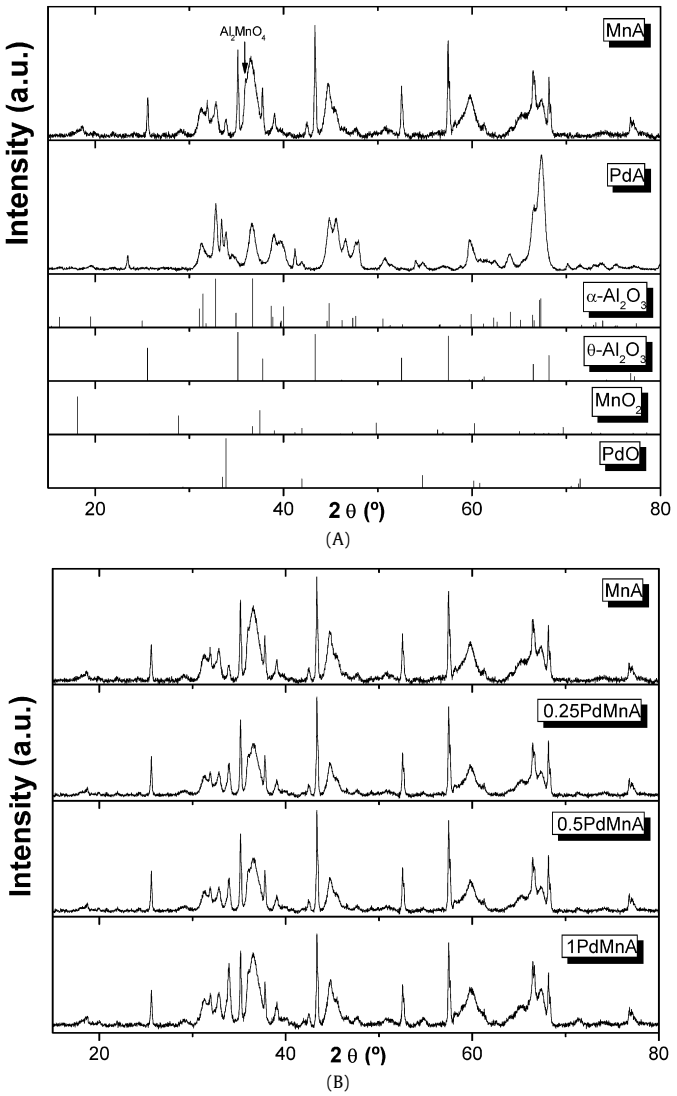

Fig. 1. X-ray diffraction patterns of: (A) Mn and Pd monometallic catalysts and (B) Mn monometallic and Mn–Pd bimetallic catalysts.

were mainly θ-Al_2O_3 monoclinic phase (JCPDS 79-1559) and cubic γ-Al_2O_3 phase (JCPDS 01-1308), with a lower contribution. For the Pd monometallic system, θ-Al_2O_3 monoclinic is also the major observed phase, with a low contribution of cubic γ-Al_2O_3 phase (JCPDS 80-0786). On the other hand, rhombohedral α-Al_2O_3 phase (JCPDS 80-0786) and monoclinic θ-Al_2O_3 phase were found in the mono- and bimetallic Mn-based catalysts. Manganese (IV) oxide (MnO_2, JCPDS 81-1947) is the major manganese-containing crystalline phase observed for MnA and the bimetallic catalysts. The presence of other manganese oxide phases such as Mn_2O_3 and Mn_3O_4 cannot be ruled out, but the characteristic diffraction lines are very difficult to match, since these phases fit with the diffraction peaks of alumina. PdO oxide is detected by XRD analysis in PdA and *x*PdMnA ($x = 0.25$ to 1) samples. An increase in the intensity of the most important diffraction lines has been found at 33.8° (101 plane) and 54.8° (112 plane) with increasing Pd content.

3.1.2. XPS

The chemical state of Mn and Pd (in the mono- and bimetallic systems) and the relative surface proportion of the elements over the alumina substrate were studied by XPS for all the catalyst samples. The binding energies of Mn $2p_{3/2}$ and Pd $3d_{5/2}$ core-levels are compiled in Table 2. All the binding energies of the Mn $2p_{3/2}$ peak

Table 2
Core electron binding energies (eV) of alumina-supported mono- and bimetallic Mn–Pd samples.

Catalyst	Al 2p	Mn $2p_{3/2}$	Pd $3d_{5/2}$	O 1s
MnA	74.5	641.9	–	531.3
0.25PdMnA	74.5	641.9	337.0	531.4
0.50PdMnA	74.5	642.0	337.1	531.3
1PdMnA	74.5	641.9	337.0	531.3
PdA	74.5	–	336.9	531.4

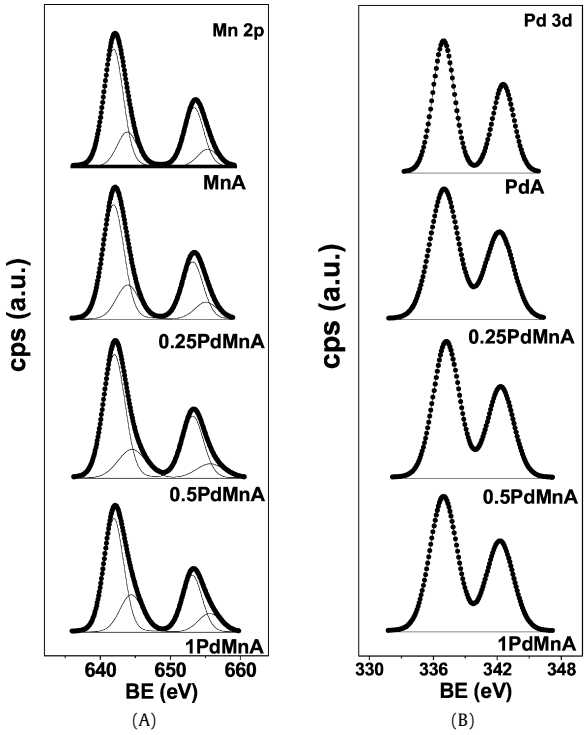

Fig. 2. (A) Mn 2p core-level spectra of MnA and *x*PdMnA catalysts; (B) Pd 3d core-level spectra of PdA and *x*PdMnA catalysts.

Table 3
Surface atomic ratios for alumina-supported mono- and bimetallic Mn–Pd samples derived from photoelectron spectroscopy.

Catalyst	Mn/Al	Pd/Al	Pd/Mn
MnA	0.25	–	–
0.25PdMnA	0.25	0.004	0.015
0.50PdMnA	0.42	0.008	0.019
1PdMnA	0.49	0.011	0.022
PdA	–	0.006	–

for the monometallic MnA and for the bimetallic *x*PdMnA fresh samples were similar and close to 641.9 eV (Fig. 2). As the Mn $2p_{3/2}$ binding energies of Mn^{3+} do not differ substantially from that of Mn^{4+}, the conclusion derived from XPS is that Mn^{3+} and Mn^{4+} species seem to coexist on the surface of the catalysts. On the other hand, the XPS analysis for the Pd systems shows that binding energies of Pd $3d_{5/2}$ peak (Table 2) are conclusive in the presence of PdO species on the catalyst surface.

The Mn/Al, Pd/Al and Pd/Mn surface ratios are presented in Table 3. An increase is observed in Pd surface exposition on both alumina and manganese oxide phases with Pd content, indicating a deposition of palladium over both alumina and manganese oxide phases. These data show that the Pd-free sample (MnA) exhibits the lowest Mn/Al ratio which is higher for the 0.50PdMnA and 1PdMnA catalysts. This finding could be due to a preferential deposition of palladium particles over alumina and/or to some dis-

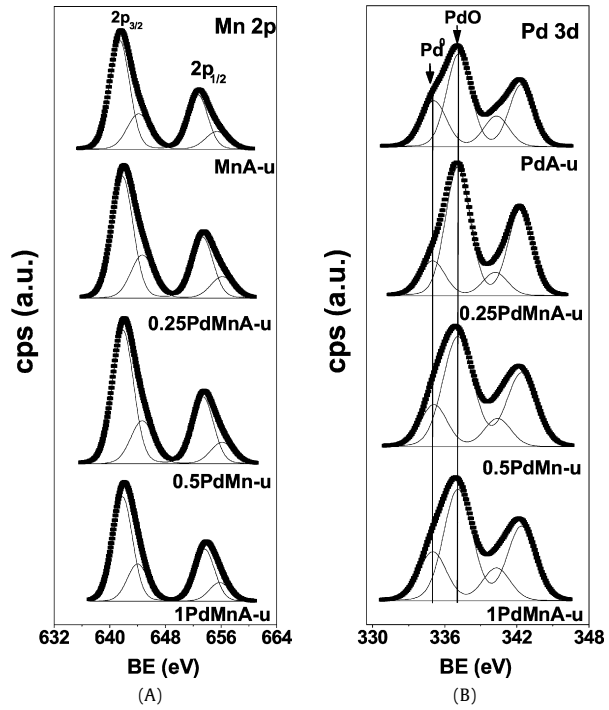

Fig. 3. (A) Mn 2p core-level spectra of MnA and *x*PdMnA used catalysts; (B) Pd 3d core-level spectra of PdA and *x*PdMnA used catalysts.

Table 4
Core electron binding energies (eV) of used alumina-supported mono- and bimetallic Mn–Pd samples.

Catalyst	Al 2p	Mn $2p_{3/2}$	Pd $3d_{5/2}$	O 1s
MnA-u[a]	74.5	641.7	–	531.2
0.25PdMnA-u	74.5	641.8	335.0 (29) 337.1 (71)	531.4
0.50PdMnA-u	74.5	641.9	335.1 (25) 337.1 (75)	531.4
1PdMnA-u	74.5	641.9	335.0 (21) 337.1 (79)	531.4
PdA-u	74.5	–	335.1 (34) 337.2 (66)	531.3

[a] The catalysts used in reaction are designated as *x*PdMnA-u (where *x* stands for the palladium loading as wt%).

aggregation of manganese particles during palladium impregnation given the acidity of the nitrate palladium solution (pH ≈ 2), since the pH of the solution decreases as Pd content increases.

XPS analysis was also performed on Mn and Mn–Pd used catalysts (Fig. 3). The photoelectron binding energies of Mn $2p_{3/2}$ and Pd $3d_{5/2}$ core-levels are compiled in Table 4. All the binding energies of the Mn $2p_{3/2}$ peak for the monometallic MnA and for the bimetallic *x*PdMnA ($x = 0.25$ to 1) used catalysts have similar values to those obtained for the fresh samples, showing that the reaction does not change the net oxidation state of Mn species. Furthermore, besides PdO, a certain proportion of metal palladium species (Pd^0) was found on the catalyst surface after reaction. As observed in previous works [15,16], the presence of manganese oxide stabilizes PdO against reduction to Pd^0 under reaction conditions.

As the Mn $2p_{3/2}$ binding energies of Mn^{3+} do not differ substantially from that of Mn^{4+}, we followed the approach of Galakhov et al. [17] to probe the valence state of manganese ions in the catalysts by studying the Mn 3s energy region. The splitting of the Mn 3s core-level spectra originates from the exchange coupling between the Mn 3s hole and Mn 3d electrons. The magnitude of this splitting is proportional to $(2S + 1)$, where S is the local spin of the 3d electrons in the ground state [18].

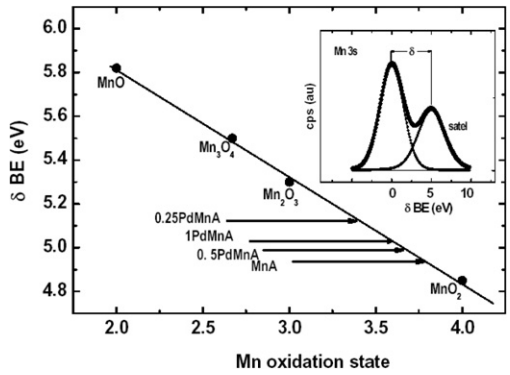

Fig. 4. Dependence of the relative energy between the Mn 3s main peak and its satellite on the formal oxidation state of manganese in pure MnO_x oxides and catalysts. The inset Mn 3s spectrum and satellite show how the magnitude of the splitting (δ BE) is measured.

Table 5
Surface atomic ratios for used alumina-supported mono- and bimetallic Mn–Pd samples derived from photoelectron spectroscopy.

Catalyst	Mn/Al	Pd/Al	Pd/Mn
MnA-u[a]	0.44	–	–
0.25PdMnA-u	0.50	0.007	0.013
0.50PdMnA-u	0.43	0.010	0.023
1PdMnA-u	0.41	0.016	0.039
PdA-u	–	0.006	–

[a] The catalysts used in reaction are designated as *x*PdMnA-u (where *x* stands for the palladium loading as wt%).

We have firstly recorded the Mn 3s spectra of MnO, Mn_3O_4, Mn_2O_3 and MnO_2 pure oxides and measured their splitting values. As shown in Fig. 4, the Mn 3s spectrum of MnO displays the largest splitting among all these oxides, and on going from MnO to MnO_2 the magnitude of the splitting decreases linearly. In the next step we have measured the Mn 3s splitting for MnA and *x*PdMnA catalysts and the corresponding values are indicated by arrows in Fig. 4. From this plot it is clear that the manganese is in an oxidation state between +3 and +4. The extreme cases are MnA and 0.25PdMnA catalysts whose δ BE values of Mn 3s level correspond to manganese formal oxidation states of +3.76 and +3.37, respectively. These new measurements, which agree with our previous conclusions derived from the analysis of Mn 2p core-level spectra, strongly support that Mn^{3+} and Mn^{4+} coexist on the surface of the catalysts, in accordance also with the results obtained by XRD.

Surface atomic ratios were also calculated for the samples used in the reaction (Table 5). As observed, Pd/Al ratios for bimetallic catalysts increase in relation to those corresponding to fresh counterparts. However, an increase in the Mn/Al ratio is observed for used catalysts with a Pd content equal to, or lower than, 0.5% and a decrease for catalysts with greater Pd content. This behavior produces a slight decrease in the Pd/Mn ratio for the used bimetallic sample with 0.25 wt% Pd and an increase for systems with a higher Pd content. The high increase in the Mn/Al ratio for used MnA and 0.25PdMnA samples in relation to fresh counterparts could be related to a preferential formation of strongly adsorbed species over alumina during reaction that decrease the Al 2p signal, increasing Pd/Al ratios in all bimetallic samples and the Mn/Al ratio in samples with a high alumina surface exposition. In this regard, it has been reported that aldol condensation reactions during the combustion of ketones in the presence of supported Mn and Pd catalysts may lead to the formation of strongly bound surface compounds [19–21]. This seems to be a general feature of carbonyl compounds carrying hydrogen atoms at their α position when ad-

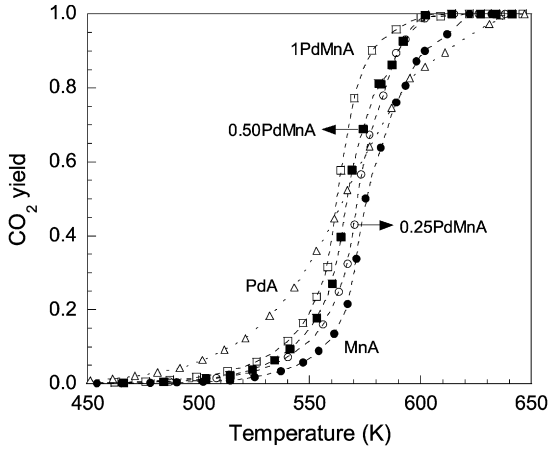

Fig. 5. Ignition curves for MEK combustion in air ($P_{MEK,0} = 126.6$ Pa; 1250 ppmv; WHSV = 425 h^{-1}) over the Pd–Mn series of catalysts: MnA (●), 0.25PdMnA (○), 0.50PdMnA (■), 1PdMnA (□) and PdA (△).

sorbed on the surface of metal oxide-based catalysts with suitable acid–base properties, as pointed out by Busca et al. [22].

3.2. Catalytic performance: ignition curves

The ignition curves for MEK combustion over the Pd–Mn/Al_2O_3 series of catalysts are shown in Fig. 5. Curves are depicted as CO_2 yield (moles of MEK converted into CO_2/moles of MEK fed into the reactor) versus reaction temperature. If the results obtained at relatively low MEK conversion are considered, it is clear that the activity increases with Pd content. In fact, taking T_{10} as the temperature at which CO_2 yield is 10%, this temperature decreases as follows: 555 K (MnA) > 546 K (0.25PdMnA) > 543 K (0.50PdMnA) > 538 K (1PdMnA) > 516 K (PdA). Thus, in the range of relatively low temperatures, the monometallic Pd/Al_2O_3 catalyst is the most active in the series. However, this situation changes at higher temperatures (and MEK conversions), as can be seen from the values of T_{90} (temperature at which the CO_2 yield is 90%): 613 K (PdA) > 602 K (MnA) > 590 K (0.25PdMnA ≈ 0.50PdMnA) > 578 K (1PdMnA). This means that in the range of relatively high reaction temperatures, the bimetallic 1PdMnA sample becomes the most active catalyst. Of course, this is the catalyst with the highest load of metal oxides, but the differences between the performance at low and high temperatures would suggest some type of cooperative effect between MnO_x and PdO_x species in these catalytic systems [12,16]. As seen in Fig. 5, the shape of the ignition curve obtained with the PdA catalyst differs notably from those of the other catalyst. Indeed, as previously mentioned, whereas its shape shows a higher activity at relatively low temperatures (and MEK conversions), the activity is less favored by the increase in temperature and/or much more detrimentally affected by the decrease in MEK concentration than for the other catalysts. This behavior indicates (*vide infra*) that the apparent activation energy and reaction order for MEK are lower and higher, respectively, over PdO_x than MnO_x.

At the weight hourly space velocity of 425 h^{-1} and MEK concentration in air of 1250 ppmv considered in this work, the Pd–Mn/Al_2O_3 catalysts allow for the complete oxidation of MEK into CO_2 at 620 K, whereas a higher temperature of 643 K is required in the case of the monometallic Pd/Al_2O_3. For the purpose of comparison with previous studies, Pina et al. [23] reported the complete combustion of 1750 ppmv of MEK at 473 K over a catalytic membrane containing 0.17 wt% Pt. Irusta et al. [24] obtained 100% conversion of 1600 ppmv of MEK in air and WHSV of 178 h^{-1} at 548 and 573 K over lanthanum-based Mn and Co perovskites, respectively. In previous papers, we reported the complete conversion of 467 ppmv of MEK in air in the 600–650 K range over a commercial 0.5 wt% Pt on alumina catalyst at WHSV of 145–582 h^{-1} [11], and 100% conversion of 600 ppmv of MEK at 580–640 K over 2.3 wt% Pt catalysts supported on pillared clays at WHSV of 432 h^{-1} [20]. In short, as concerns the light-off curves, the performance of the Pd–Mn/Al_2O_3 catalysts is similar to that of supported Pt catalysts under comparable MEK concentration and space velocity conditions.

3.3. Catalytic performance: formation of partially oxidized products

The question of the possible formation of partial oxidation products is a very important issue in catalytic combustion, since this technology is intended for the complete oxidation of VOCs or methane to CO_2 and H_2O, whereas the presence of partially oxidized products in flue gases could give rise to environmental and health concerns. Regarding the combustion of MEK over supported Pt catalysts, 100% selectivity for the complete oxidation products was found in previous works [11,20]. However, when using Pd–Mn/Al_2O_3 catalysts, acetaldehyde, methyl-vinyl-ketone, diacetyl and trace amounts of acetic acid are also formed. Fig. 6 shows the yields (moles of MEK converted into a given product/moles of MEK fed into the reactor) of the main reaction products obtained with the MnA, 0.50PdMnA (a representative bimetallic catalyst) and PdA catalysts. The lowest formation of partially oxidized products takes place over the monometallic Pd catalyst, with maximum yields of acetaldehyde and methyl-vinyl-ketone below 1% and even lower yields of diacetyl. However, in presence of manganese oxides, the formation of these products is favored at low and intermediate MEK conversion levels. With the MnA and 0.50PdMnA catalysts, maximum yields of acetaldehyde, diacetyl and methyl-vinyl-ketone were 5–6%, 2–2.5% and 0.5–1%, respectively. The presence of a higher or lower amount of Pd, as in the 1PdMnA and 0.25PdMnA catalysts, does not substantially change these values, which points to manganese species as the one mainly responsible for MEK partial oxidation. The yields of acetaldehyde, methyl-vinyl-ketone and diacetyl increase with reaction temperature, passing through a maximum value near the ignition point, and then decreasing to become zero at higher temperatures, when selectivity to CO_2 is 100%. This can be clearly seen in Fig. 7, where the evolution of the yields is plotted against MEK conversion. Irrespective of the catalyst, maximum acetaldehyde and diacetyl yields are attained at about 50 and 30% MEK conversion, respectively. The situation is more complex in the case of methyl-vinyl-ketone. The maximum yield of this product is attained at low conversion (20%) over PdA, whereas it is shifted to 50% MEK conversion in the presence of manganese species.

Diacetyl is an interesting naturally-occurring vicinal diketone that is used in the food and beverage industries because of its characteristic buttery flavor. A number of papers have been dedicated to the direct synthesis of diacetyl through the partial oxidation of MEK [25–30]. This reaction is also of interest from a core perspective, since it represents the functionalization of a molecule at a carbon atom in the α position of an existing carbonyl group. McCullagh et al. [28,30] proposed a general reaction network for the oxidation of MEK that, adapted to the conditions relevant in catalytic combustion where CO_2 and H_2O are ultimately produced, is schematized in Fig. 8. The scheme is complex and includes 4 main reaction pathways in parallel. The first one is the formation of diacetyl and methyl-vinyl-ketone from a common reaction intermediate that was identified as acetoin (3-hydroxybutan-2-one) [30]. The second pathway is the direct complete oxidation of MEK. The third and fourth reaction pathways give rise to the formation of acetaldehyde and acetic acid. Intermediate 2 (Fig. 8) has been reported to be a diol (butane-2,3-diol), which is oxidatively cleaved to form 2 molecules of acetaldehyde [28]. The inclusion of this reaction is important because it explains the larger pro-

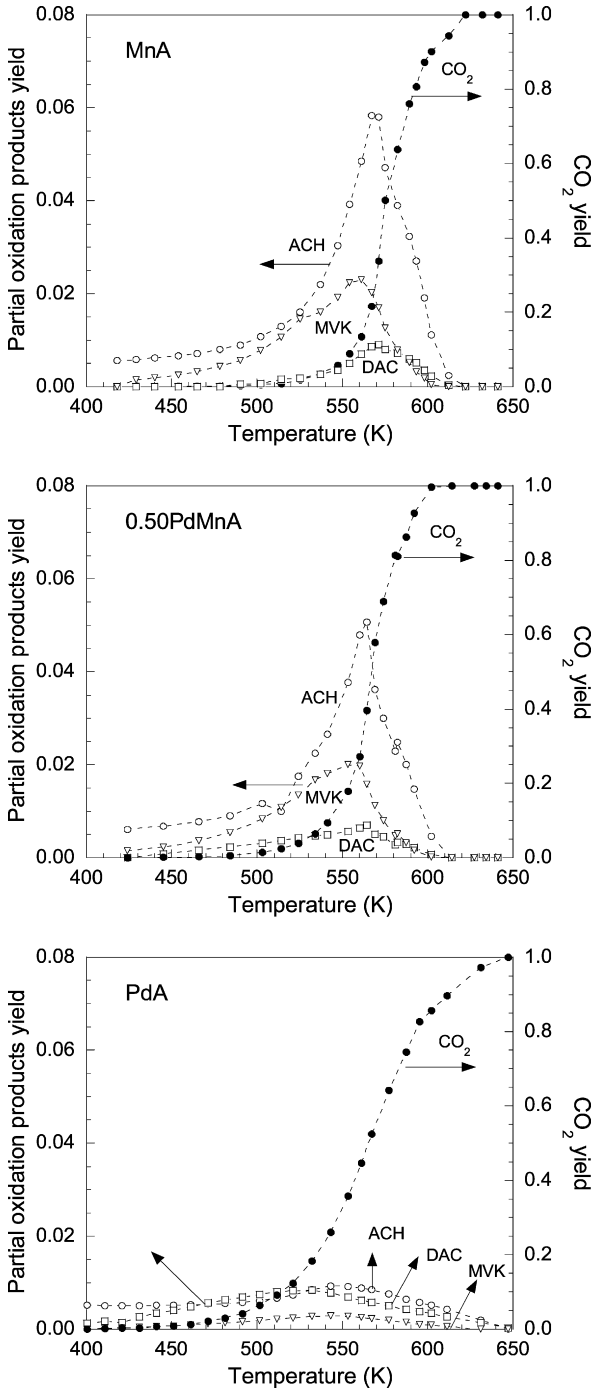

Fig. 6. Yields of the MEK oxidation products ($P_{MEK,0}$ = 126.6 Pa, 1250 ppmv; WHSV = 425 h^{-1}) as a function of reaction temperature over the MnA, 0.50PdMnA and PdA catalysts: CO_2 (●), acetaldehyde (○, AC), methyl-vinyl-ketone (▽, MVK) and diacetyl (□, DAC).

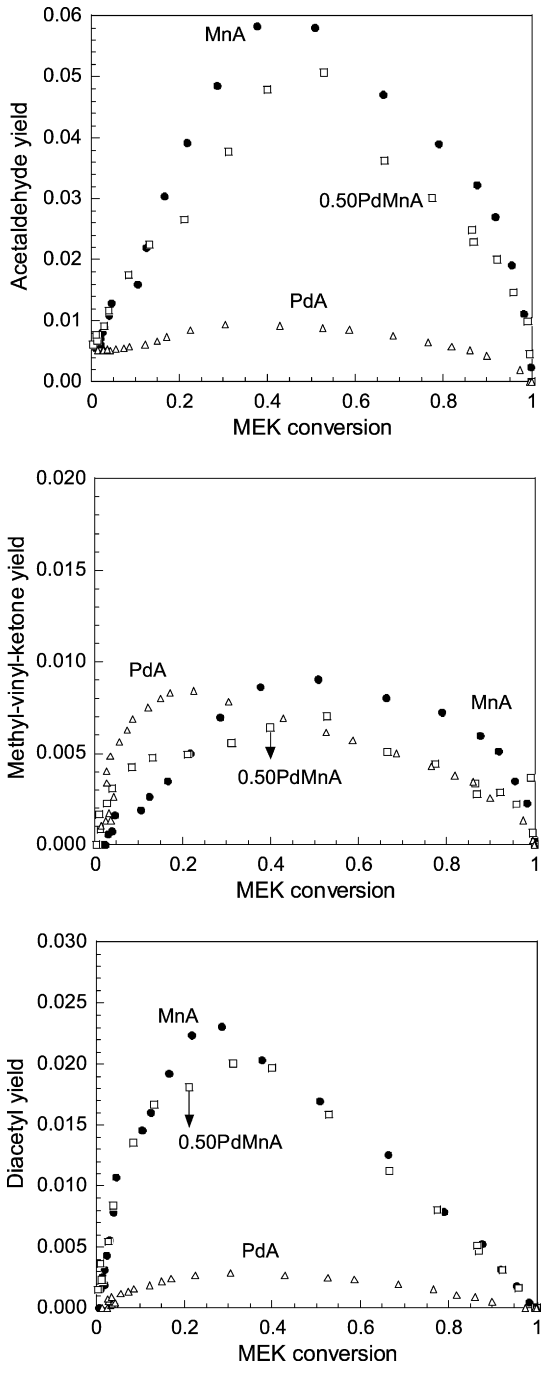

Fig. 7. Yields of the MEK oxidation products ($P_{MEK,0}$ = 126.6 Pa, 1250 ppmv; WHSV = 425 h^{-1}) as a function of MEK conversion over the MnA (●), 0.50PdMnA (□) and PdA (△) catalysts.

portion of acetaldehyde compared to acetic acid that is typically obtained in spite of the fact that the acid is more difficult to oxidize than the aldehyde. Finally, Intermediate 3 (Fig. 8) is the enol form of MEK ($CH_3COH{=}CHCH_3$), which is oxidized to acetaldehyde and acetic acid. According to McCullagh et al. [28], the participation of this intermediate has to be included in any mechanism of MEK oxidation, especially at high oxygen partial pressures. Takita et al. [26,27] found that basic oxides (Co_3O_4, NiO) promoted the formation of diacetyl, whereas the acidic ones (V_2O_5, MoO_3, WO_3, Cr_2O_3) mainly catalyzed the scission reactions to C_2 moieties.

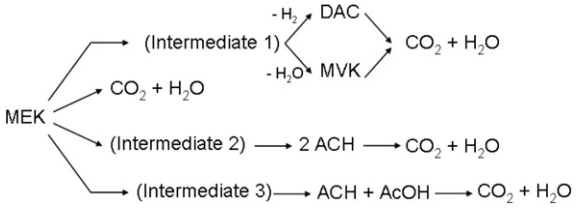

Fig. 8. Reaction network for methyl-ethyl-ketone (MEK) oxidation: diacetyl (DAC), methyl-vinyl-ketone (MVK), acetaldehyde (ACH) and acetic acid (AcOH). Scheme adapted from McCullagh et al. [28,30].

The results of this study are basically consistent with the above-described reaction network. As shown in Fig. 6, at low reaction temperatures below 450 K there is practically no production of CO_2, and the only reaction products are acetaldehyde and diacetyl over the Mn-containing catalysts, and acetaldehyde and methyl-vinyl-ketone over the monometallic Pd catalyst. As the temperature increases, the yield of all the reaction products increases, until a maximum yield for MEK partial oxidation products is achieved at MEK conversions between 20 and 50% depending on the catalyst and the reaction product being considered. On the other hand, the rate of the reactions leading to CO_2 production from MEK and the partially oxidized compounds is more favored by the increase in temperature. As a result, the yield of CO_2 increases continuously until this carbon oxide becomes the only reaction product at temperatures in the 620–643 K range. The main difference between the results of this study and previous reports on MEK partial oxidation is perhaps the extremely low amounts of acetic acid produced by the Pd–Mn/Al_2O_3 catalysts. On the other hand, none of the intermediate products has been detected with our analysis method. This seems to be influenced by the very low MEK concentration and large oxygen excess prevailing in our experimental conditions that favor the scission and combustion reactions instead of the partial oxidation preserving the carbon skeleton; as well as, of course, by the catalyst nature. As a matter of fact, MEK combustion on Pt catalysts under similar reaction conditions proceeds with the sole production of CO_2 [11,20]. Regarding acetic acid, it should be noted that this product comes from the cleavage of the enol form of MEK (Fig. 8). It seems likely that the complete oxidation of this intermediate is easy under our reaction conditions, thereby leading to an undetectable acetic acid production. This would indicate that the cleavage of the diol intermediate (butane-2,3-diol) is the main source of acetaldehyde. Ketones record high chemical reactivity on metal oxides, and species such as enolates and carboxylates have been identified upon their adsorption on transition metal oxides [22,31,32], alumina [33,34] and silica [35,36]. These species, as well as alkoxides, are considered to be involved in the reaction pathways leading to the combustion of hydrocarbons [22,32,37,38]. In our case, the role of the support cannot be discarded. In fact, acetone interacts with Lewis acid sites of γ-Al_2O_3 through the oxygen atom to form an enol that is considered to be the intermediate in the carbon–carbon bond scission producing CO_2 and H_2O at high temperatures [33,34]. Reed et al. [39] have proposed that the migration of adsorbed acetone intermediates from the silica support to Mn sites is involved in the mechanism of the complete oxidation of this ketone with ozone on MnO_x/SiO_2 catalysts.

3.4. MEK combustion kinetics

This kinetic study is based on the data of CO_2 formation rate (R_{CO_2}) obtained at steady state, operating the reactor under a differential regime of MEK conversion ($X_{MEK} < 0.15$) and calculated according to

$$(R_{CO_2}) = \frac{4 \cdot Y_{CO_2}}{(W/F_{MEK,0})}, \tag{1}$$

where Y_{CO_2} is the measured yield of CO_2 (moles of MEK converted into CO_2/moles of MEK fed into the reactor) and $W/F_{MEK,0}$ the space–time referred to the amount of catalyst loaded into the reactor (W) and the MEK molar flow rate in the reactor feed ($F_{MEK,0}$). In these experiments the selectivity for CO_2 was always above 60%.

3.4.1. Power-law rate model

Our first approach was to consider an empirical power-law (PL) rate model

$$(R_{CO_2}) = k_{PL} \cdot P_{MEK}^{\alpha}, \tag{2}$$

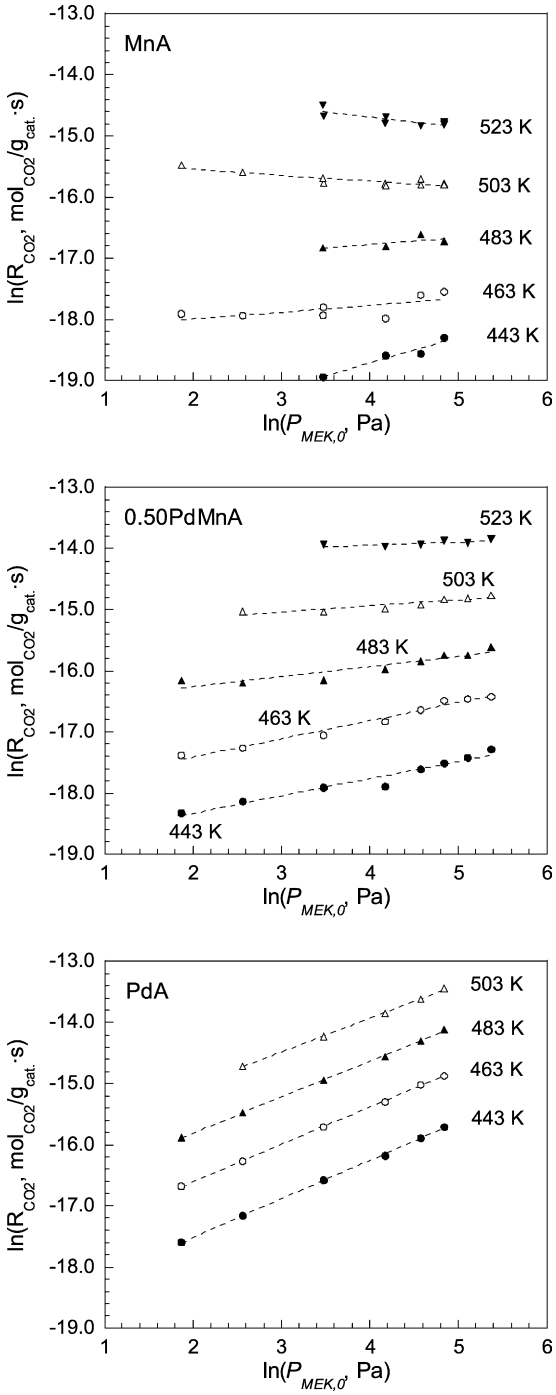

Fig. 9. Power-law rate model plot for the production of CO_2 from MEK combustion over the MnA, 0.50PdMnA and PdA catalysts at the indicated temperatures.

$$\ln(R_{CO_2}) = \ln k_{PL} + \alpha \cdot \ln P_{MEK}, \tag{3}$$

where k_{PL} is the kinetic constant of the power-law model which includes dependence on the oxygen partial pressure that can be assumed constant, since oxygen is in considerable excess with respect to the stoichiometrically necessary amount. P_{MEK} is the MEK partial pressure and α the apparent reaction order for MEK. A plot of the natural logarithms of R_{CO_2} and P_{MEK}, including the results obtained with the catalysts MnA, 0.50PdMnA and PdA is shown in Fig. 9. As can be seen, the power-law model fits well the data obtained with the monometallic Pd catalyst. In the case of the catalysts containing Mn, the fit is also reasonable, but a dependence of the apparent reaction order for MEK on the reaction temper-

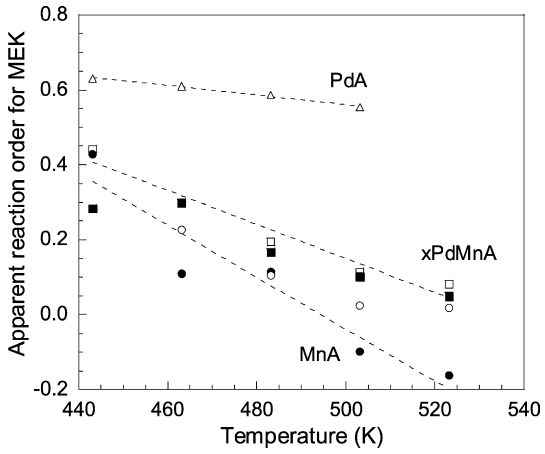

Fig. 10. Apparent reaction orders for MEK (α) according to the power-law kinetic model for the combustion of MEK over the Pd–Mn series of catalysts: MnA (●), 0.25PdMnA (○), 0.50PdMnA (■), 1PdMnA (□) and PdA (△).

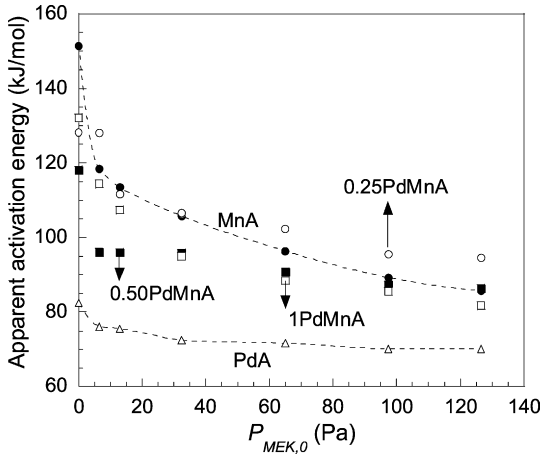

Fig. 11. Apparent activation energy according to the power-law kinetic model for the combustion of MEK over the Pd–Mn series of catalysts: MnA (●), 0.25PdMnA (○), 0.50PdMnA (■), 1PdMnA (□) and PdA (△).

ature can be appreciated from the change in the slope of the straight lines. This effect is more clearly shown in Fig. 10, where the value of α is displayed as a function of the reaction temperature for the three representative catalysts. Only in the case of the monometallic Pd catalyst does the apparent reaction order remain relatively unaffected, with a value of about 0.6. In contrast, α decreases with reaction temperature from around 0.4 at 443 K to values close to 0 over the bimetallic *x*PdMnA catalysts and even to negative values (−0.2) over the monometallic Mn catalyst at 523 K. On the other hand, the corresponding Arrhenius plots show that the apparent activation energy for MEK combustion decreases when MEK partial pressure increases in the range of low concentration of the ketone, as shown in Fig. 11. In the case of the PdA catalyst, this parameter remains almost constant, but the variation for the Mn-containing samples is remarkable. Taking, for example, $P_{MEK} = 126.6$ Pa (1250 ppmv) as reference, the resulting values are 70 kJ/mol for PdA, 82 kJ/mol for 1PdMnA, 86 kJ/mol for MnA and 0.50PdMnA and 95 kJ/mol for 0.25PdMnA. Clearly, the monometallic Pd catalyst provides the lowest apparent activation energy, with a value very similar to the one obtained for a 0.5 wt% Pt/Al_2O_3 catalyst, also with a power-law kinetic model (73 kJ/mol, $P_{MEK} = 191$ Pa) [11]. Higher values are obtained for the catalysts containing MnO_x, which is also in line with results previously reported by other researchers for MEK combustion over transition metal oxides as Fe_2O_3 (117 kJ/mol) [9].

In spite of the fact that the variation of the kinetic parameters with the composition and temperature renders the power-law model invalid, the results obtained can be considered as indicative of catalyst features. Actually, the results provided by this model explain the differences among the ignition curves described in Section 3.2 (Fig. 5). As mentioned earlier, the lowest apparent activation energy corresponds to PdA, whereas the apparent reaction order for MEK is much lower over the Mn-containing catalysts than over the monometallic Pd sample. The combination of these effects explains the relatively good performance shown by the bimetallic Pd–Mn catalysts at high values of MEK conversion resulting in lower temperatures to achieve complete combustion, and also the superior performance of PdA at relatively low temperatures. The fact that PdA is the sample best described by the power-law model can be related to the high selectivity of this catalyst towards complete oxidation products. In the case of the Mn-containing catalysts, CO_2 and water are probably produced from a variety of substrates. As a result, it is not striking that a simple expression like Eq. (2) provides worse results with the least selective catalysts.

3.4.2. Mars–van Krevelen and Langmuir–Hinshelwood models

In a previous work, we found that the kinetics of the combustion of MEK in air at low concentrations over a Pt/Al_2O_3 catalyst is well described by both the first-order Mars–van Krevelen (MvK) rate equation and a Langmuir–Hinshelwood (LH) kinetic expression, derived from a mechanism assuming surface reaction between MEK and atomic oxygen adsorbed on the same type of sites as the rate-determining step [11]. These rate equations can be written as follows:

$$(R_{CO_2})_{MvK} = \frac{k_{MvK} \cdot P_{MEK}}{1 + \frac{\nu \cdot k_{MvK}}{k_{ox} \cdot P_{O_2}} \cdot P_{MEK}} = \frac{k_{MvK} \cdot P_{MEK}}{1 + k'_{MvK} \cdot P_{MEK}}, \quad (4)$$

$$(R_{CO_2})_{LH} = \frac{k_{LH} \cdot K_{MEK} \cdot \sqrt{K_{O_2} \cdot P_{O_2}} \cdot P_{MEK}}{(1 + K_{MEK} \cdot P_{MEK})^2} = \frac{k'_{LH} \cdot P_{MEK}}{(1 + K_{MEK} \cdot P_{MEK})^2}, \quad (5)$$

where k_{MvK} and k_{ox} are the kinetic constants of MEK combustion and catalyst reoxidation steps according to the Mars–van Krevelen mechanism, and ν is the stoichiometric coefficient of O_2 for MEK combustion (5.5). On the other hand, k_{LH} is the kinetic constant of the surface reaction, which is the rate-determining step in the Langmuir–Hinshelwood mechanism adopted; K_{MEK} and K_{O_2} are the equilibrium constants for the adsorption of MEK and oxygen, respectively. These kinetic models have also been considered in this study, and fittings of the rate data to Eqs. (4) and (5) are shown in Fig. 12 as dotted and solid lines, respectively. As in the case of Pt, kinetic data from the monometallic Pd catalyst are satisfactorily described by both MvK and LH kinetic models. However, for the Mn-containing catalysts, fitting to the surface redox Mars–van Krevelen model is the best at very low MEK partial pressures. Estimated kinetic and statistical parameters for all the catalysts are included in Table 6. The statistical parameters evaluated have been the model selection criterion (MSC) and the coefficient of determination (DC) [9]. As it can be seen, the values of MSC and DC are consistently higher for the Mars–van Krevelen than for the Langmuir–Hinshelwood model, especially for the bimetallic Pd–Mn catalysts. However, these results of rate data fitting are not conclusive regarding the reaction mechanism. In fact, a recent paper by Vannice [40] shows that the original derivation of the Mars–van Krevelen rate equation is inconsistent and that it has no physical relevance. Moreover, rate expressions derived from more realistic Langmuir–Hinshelwood models can fit the kinetic data as well as or even better than the Mars–van Krevelen rate equation. Indeed,

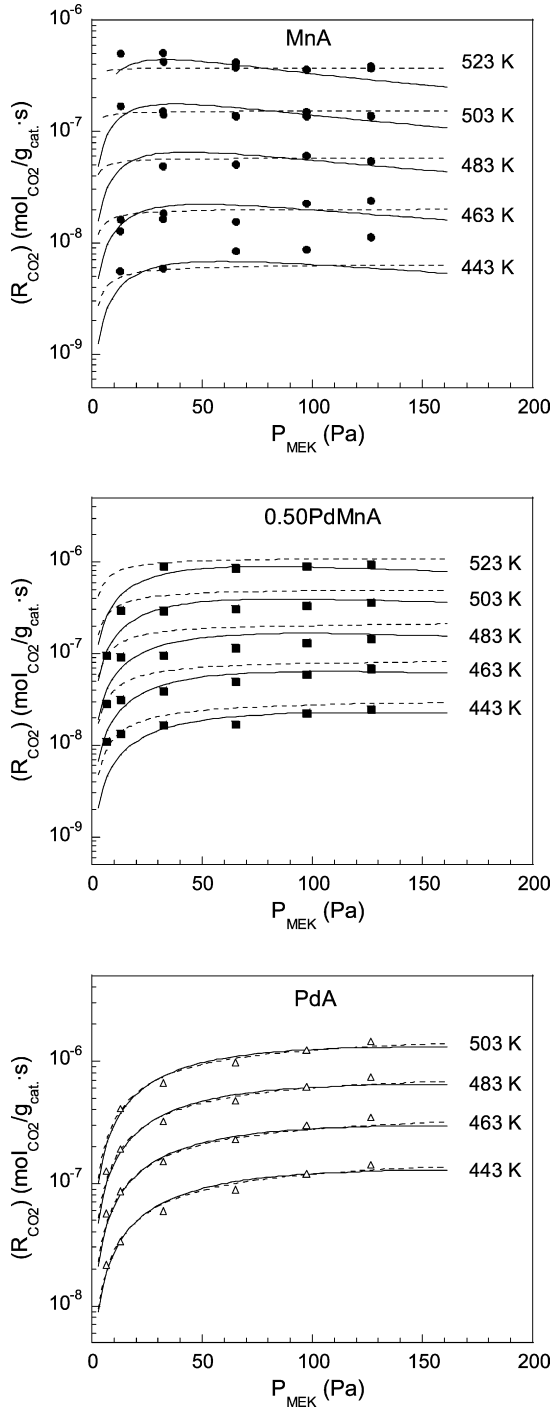

Fig. 12. Rates of CO_2 formation for MEK as a function of MEK partial pressure at the indicated temperatures. Points are experimentally obtained values with the MnA (●), 0.50PdMnA (■) and PdA (△) catalysts. Dotted and solid lines correspond to the fitting of the kinetic data to the Mars–van Krevelen (Eq. (4)) and Langmuir–Hinshelwood (Eq. (5)) rate equations, respectively.

a LH model including the reaction between oxygen from the gas phase and adsorbed MEK can lead to a rate equation that is mathematically equivalent to the MvK one that fits the kinetic data equally well [11]. In our case, irrespective of the model, MvK or LH, the values of the kinetic parameters for the bimetallic Pd–Mn catalysts are intermediate between the values for the monometallic MnA and PdA samples. This can be clearly illustrated by analyzing the results for the activation energy (E_{MvK}). This parameter adopted 76 kJ/mol for the PdA catalyst, close to the value given by

Table 6
Estimated kinetic and statistical[a] parameters of the Mars–van Krevelen (MvK) and Langmuir–Hinshelwood (LH) rate equations for the combustion of MEK over the catalysts indicated.[b]

Parameter	MnA	0.25PdMnA	0.50PdMnA	1PdMnA	PdA
$k_{MvK} \times 10^8$ [mol/(g_{cat} Pa s)]	2.2	1.5	1.0	1.4	1.2
k'_{MvK} [Pa^{-1}]	0.62	0.21	0.10	0.10	0.02
E_{MvK}[c] [kJ/mol]	152	133	115	117	76
$k'_{LH} \times 10^8$ [mol/(g_{cat} Pa s)]	0.3	0.4	0.4	0.7	1.1
K_{MEK} [Pa^{-1}]	0.021	0.015	0.010	0.014	0.006
E_{LH}[d] [kJ/mol]	114	108	99	94	75
$-\Delta H_{MEK,LH}$[e] [kJ/mol]	14	10	11	2.0	3.0
MSC_{MvK}	18.0	137.6	35.1	44.7	70.8
MSC_{LH}	15.0	34.7	19.7	43.5	47.4
DC_{MvK}	0.962	0.995	0.990	0.992	0.986
DC_{LH}	0.949	0.973	0.963	0.987	0.979

[a] The statistical parameters considered are the model selection criterion (MSC) and the coefficient of determination (DC).
[b] Values of the kinetic and equilibrium constants are given at 473 K.
[c] Activation energy for MEK combustion according to the Mars–van Krevelen model.
[d] Activation energy for MEK combustion according to the Langmuir–Hinshelwood model.
[e] Enthalpy for MEK adsorption according to the Langmuir–Hinshelwood model.

the power-law model (70 kJ/mol), which also fitted the rate data well. On the other hand, E_{MvK} was as high as 152 kJ/mol for the MnA catalyst. In the case of the bimetallic samples, the activation energy was 115–117 kJ/mol for 0.50PdMnA and 1PdMnA, and increased to 133 kJ/mol for the bimetallic sample with the lowest Pd content. The kinetic constants at 473 K of the two models, k_{MvK} and k'_{LH}, are similar to each other and from sample to sample. In contrast, the enthalpy and equilibrium constant for MEK adsorption are much higher over Mn than Pd species, which indicates a greater affinity between MEK and manganese oxides.

The presence of a cooperative effect between palladium and manganese species in PdO_x/MnO_x catalysts for CO oxidation has been reported [41,42]. This effect was described considering that MnO_x supplied oxygen onto Pd where the oxidation reaction takes place. An improved catalytic performance was also found upon increasing the oxidation state of Mn [42]. Requies et al. [16] have also found a positive effect in the presence of Mn species that increased the stability of PdO during methane combustion over Pd–Mn monolith catalysts. However, this reaction is conducted at much higher temperatures that the ones required for MEK combustion. In our case, the XPS results revealed that the net oxidation state of Mn does not change during reaction. On the other hand, in the case of palladium, Pd^0 is found in the used samples, whereas PdO is the dominant species in the fresh catalysts. Moreover, the analysis of the Mn/Al, Pd/Al and Pd/Mn surface ratios suggests a preferential deposition of Pd onto alumina and a strong interaction of Mn with the support. This situation, together with the relatively low reaction temperatures, would render the manifestation of cooperative effects of the type described in previous reports more difficult [16,42]. Therefore, the performance in the MEK combustion reaction of the bimetallic $Pd–Mn/Al_2O_3$ catalysts in this study seems to be dominated by the additive rather than the cooperative effect of Pd^0, PdO and MnO_x species.

4. Summary and conclusions

The catalytic combustion of MEK in air at low concentrations takes place over $Pd–Mn/Al_2O_3$ catalysts with the formation of acetaldehyde, methyl-vinyl-ketone, and diacetyl as well as CO_2 and water. The partial oxidation products are formed in parallel, being favored over the Mn-containing catalysts at low and intermediate levels of MEK conversion, below the ignition point. Monometallic Pd/Al_2O_3 was the most selective catalyst for MEK complete oxidation. The only reaction products at 100% MEK conversion

were CO_2 and H_2O over all the catalysts considered in this study. MnO_2 and PdO were the most abundant species in the fresh catalysts. XPS analysis performed on the samples used after reaction revealed that whereas the oxidation state of Mn did not significantly change, both Pd^0 and PdO coexisted in the palladium-containing catalysts. In what concerns the combustion kinetics, the classical first-order redox Mars–van Krevelen (MvK) mechanism and a Langmuir–Hinshelwood (LH) model assuming the surface reaction between adsorbed MEK and oxygen as the rate-determining step, have been considered. Both models satisfactorily fitted the rates of CO_2 formation obtained with the monometallic PdO_x/Al_2O_3 catalyst. In the case of the bimetallic Pd–Mn catalysts, the MvK model provided the best fit. Irrespective of the model, the kinetic parameters for the bimetallic catalysts were in-between the values for the monometallic samples. The activation energy and MEK enthalpy of adsorption were considerably lower over PdO_x than MnO_x. The selectivity and kinetics of MEK combustion over the bimetallic catalysts is dominated by an additive rather than cooperative effect between palladium and manganese species.

Acknowledgments

G.A. and L.M.G. gratefully acknowledge the financial support for this work provided by the Spanish Ministry of Science and Innovation (MAT2006-12386-C05). M.C.A.-G. acknowledges financial support from the MCYT in the Ramón y Cajal research program.

References

[1] R.E. Hayes, S.T. Kolaczkowski, Introduction to Catalytic Combustion, Gordon and Breach Science Publishers, Amsterdam, 1997, p. 1.
[2] B.K. Hodnett, Heterogeneous Catalytic Oxidation, John Wiley & Sons, Chichester, 2000, p. 189.
[3] R. Prasad, L.A. Kennedy, E. Ruckenstein, Catal. Rev.-Sci. Eng. 26 (1984) 1.
[4] J.J. Spivey, in: G.C. Bond, G. Webb (Eds.), Catalysis, vol. 8, The Royal Society of Chemistry, Cambridge, 1989, p. 157.
[5] M.F.M. Zwinkels, S.G. Järås, P.G. Menon, T.A. Griffin, Catal. Rev.-Sci. Eng. 35 (1993) 319.
[6] F. Duprat, Chem. Eng. Sci. 57 (2002) 901.
[7] G. Ware (Ed.), Reviews of Environmental Contamination and Toxicology, vol. 103, Springer, Berlin, 1988, p. 165.
[8] J.C. Lou, C.L. Chen, Hazard. Waste Hazard. Mater. 12 (1995) 37.
[9] G. Picasso Escobar, A. Quintilla Beroy, M.P. Pina Iritia, J. Herguido Huerta, Chem. Eng. J. 102 (2004) 107.
[10] V.R. Choudary, G.M. Deshmukh, Chem. Eng. Sci. 60 (2005) 1575.
[11] G. Arzamendi, R. Ferrero, A.R. Pierna, L.M. Gandía, Ind. Eng. Chem. Res. 46 (2007) 9037.
[12] M.C. Álvarez-Galván, V.A. de la Peña O'Shea, J.L.G. Fierro, P.L. Arias, Catal. Commun. 4 (2003) 223.
[13] M.C. Álvarez-Galván, B. Pawelec, V.A. de la Peña O'Shea, J.L.G. Fierro, P.L. Arias, Appl. Catal. B: Environ. 51 (2004) 83.
[14] V.A. de la Peña O'Shea, M.C. Álvarez-Galván, J.L.G. Fierro, P.L. Arias, Appl. Catal. B: Environ. 57 (2005) 191.
[15] V.A. de la Peña O'Shea, M.C. Álvarez-Galván, J. Requies, V.L. Barrio, P.L. Arias, J.F. Cambra, M.B. Güemez, J.L.G. Fierro, Catal. Commun. 8 (2007) 1287.
[16] J. Requies, M.C. Álvarez-Galván, V.L. Barrio, P.L. Arias, J.F. Cambra, M.B. Güemez, A. Manrique Carrera, V.A. de la Peña O'Shea, J.L.G. Fierro, Appl. Catal. B: Environ. 79 (2008) 122.
[17] V.R. Galakhov, M. Demeter, S. Bartkowski, M. Neumann, N.A. Ovechkina, E.Z. Kurmaev, N.I. Labachevskaya, Ya.M. Mukoskii, J. Mitchell, D.L. Ederer, Phys. Rev. B 65 (2002) 113102.
[18] I. Barrio, I. Legórburu, M. Montes, M.I. Domínguez, M.A. Centeno, J.A. Odriozola, Catal. Lett. 101 (2005) 151.
[19] M. Paulis, L.M. Gandía, A. Gil, J. Sambeth, J.A. Odriozola, M. Montes, Appl. Catal. B: Environ. 26 (2000) 37.
[20] A. Gil, M.A. Vicente, J.-F. Lambert, L.M. Gandía, Catal. Today 68 (2001) 41.
[21] L.M. Gandía, M.A. Vicente, A. Gil, Appl. Catal. B: Environ. 38 (2002) 295.
[22] G. Busca, E. Finocchio, G. Ramis, G. Ricchiardi, Catal. Today 32 (1996) 133.
[23] M.P. Pina, S. Irusta, M. Menéndez, J. Santamaría, R. Hughes, N. Boag, Ind. Eng. Chem. Res. 36 (1997) 4557.
[24] S. Irusta, M.P. Pina, M. Menéndez, J. Santamaría, J. Catal. 179 (1998) 400.
[25] M. Ai, J. Catal. 89 (1984) 413.
[26] Y. Takita, K. Inokuchi, O. Kobayashi, F. Hori, N. Yamazoe, T. Seiyama, J. Catal. 90 (1984) 232.
[27] Y. Takita, F. Hori, N. Yamazoe, T. Seiyama, Bull. Chem. Soc. Jpn. 60 (1987) 2757.
[28] E. McCullagh, J.B. McMonagle, B.K. Hodnett, Appl. Catal. A: Gen. 93 (1993) 203.
[29] E. McCullagh, N.C. Rigas, J.T. Gleaves, B.K. Hodnett, Appl. Catal. A: Gen. 95 (1993) 183.
[30] E. McCullagh, N.C. Rigas, J.T. Gleaves, B.K. Hodnett, Stud. Surf. Sci. Catal. 82 (1994) 853.
[31] E. Finocchio, R.J. Willey, G. Busca, V. Lorenzelli, J. Chem. Soc., Faraday Trans. 93 (1997) 175.
[32] G. Busca, E. Finocchio, V. Lorenzelli, G. Ramis, M. Baldi, Catal. Today 49 (1999) 453.
[33] B.E. Hanson, L.F. Wieserman, G.W. Wagner, R.A. Kaufman, Langmuir 3 (1987) 549.
[34] V. Ermini, E. Finocchio, S. Sechi, G. Busca, S. Rossini, Appl. Catal. A: Gen. 190 (2000) 157.
[35] T. Yamaguchi, Y. Nakano, K. Tanabe, Bull. Chem. Soc. Jpn. 51 (1978) 2482.
[36] J.C. McManus, Y. Harano, M.J.D. Low, Can. J. Chem. 47 (1969) 2545.
[37] E. Finocchio, R.J. Willey, G. Ramis, G. Busca, V. Lorenzelli, Stud. Surf. Sci. Catal. 101 (1996) 483.
[38] J. Haber, Stud. Surf. Sci. Catal. 110 (1997) 1.
[39] C. Reed, Y. Xi, S.T. Oyama, J. Catal. 235 (2005) 378.
[40] M.A. Vannice, Catal. Today 123 (2007) 18.
[41] S. Imamura, Y. Tsuji, Y. Miyake, T. Ito, J. Catal. 151 (1995) 279.
[42] J.S. Park, D.S. Doh, K.-Y. Lee, Top. Catal. 10 (2000) 127.